

# **Analyses du Fender Bassman 5F6**





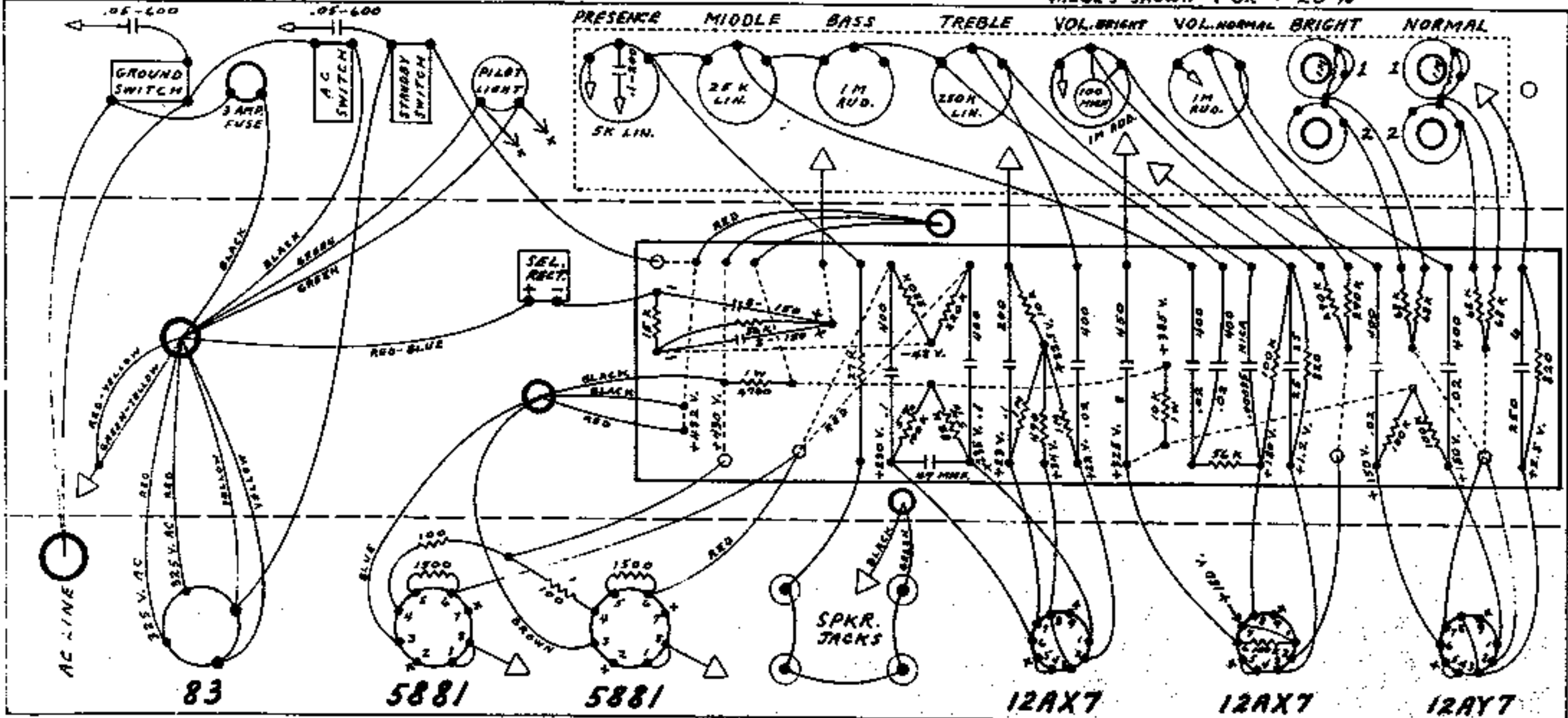
# FENDER "BASSMAN" LAYOUT

## MODEL 5F6

F-66

### NOTICE

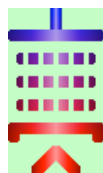
VOLTAGES READ TO GROUND  
WITH ELECTRONIC VOLTMETER  
VALUES SHOWN + OR - 20%



NOTE - ALL RESISTORS ARE ONE-HALF WATT 10% TOLERANCE UNLESS OTHERWISE NOTED







# The Fender Bassman 5F6-A Circuit

by **Richard Kuehnel**

## Pentode Press

- [Home](#)
- [Buy Our Books](#)
- [How to Contact Us](#)
- [Legal Notice](#)

## Tutorial - Tube Amp Algebra

- [Electric Charge and Electric Current](#)
- [Work, Voltage, and Power](#)
- [Georg Simon Ohm's Law](#)
- [Voltage Division](#)
- [Current Division](#)
- [Gustav Robert Kirchhoff's Voltage Law](#)
- [Kirchhoff's Current Law](#)
- [Imaginary Numbers](#)
- [Complex Impedance](#)
- [Gabriel Cramer's Rule](#)
- [Pierre-Simon Laplace, etc.](#)

## Vacuum Tube History

- [Vacuum Tube Technology Circa 1950](#)
- [The Ultralinear Amplifier](#)
- [Leo Fender's Calculations](#)

## The Fender Bassman 5F6-A

- [The 5F6-A Circuit](#)
- [Class AB Power Supply Ripple](#)
- [Bassman Chassis Photos](#)

## Tonestacks: 5F6-A vs. JMP50

- [Introduction](#)
- [Bass and Midrange Response](#)
- [Treble Response](#)
- [Creating Your Own Design](#)

## The Marshall JMP50 1987

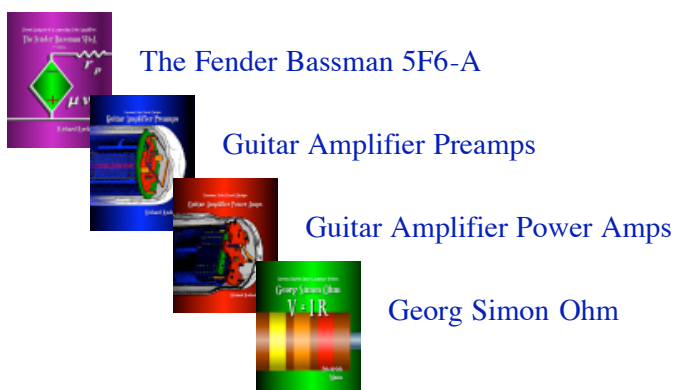
- [The First-Stage Preamp Circuit](#)
- [The Second-Stage Voltage Amp](#)
- [The Grid Bias Supply](#)
- [The Push-Pull Power Amp](#)

## Electronic Design Calculators

### Circuits and Systems

### Medieval Studies

### Living Water in Slavic Folklore



## Safety Warning

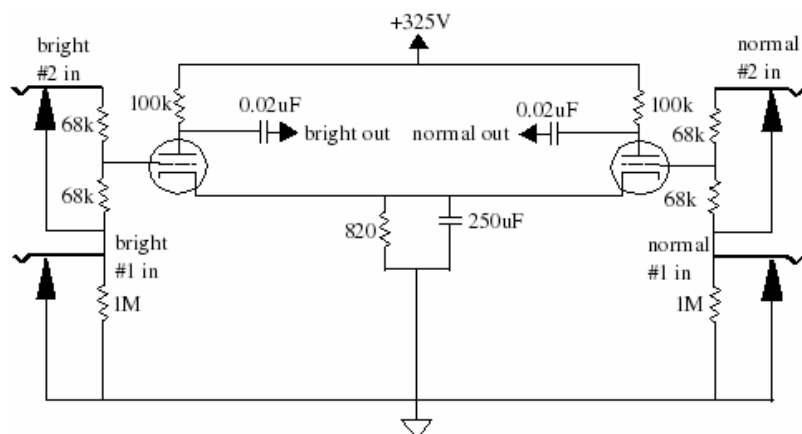
It is important to remember that vacuum tube circuits generally use lethally high voltages. Capacitors store these lethal voltages long after the amplifier has been turned off and unplugged. Please do not work on one of these circuits unless you are properly trained.

## The 1st-Stage 12AY7 Preamp

The Bassman 5F6-A preamp contains two voltage amplifiers, one for the bright inputs and one for the normal inputs. The preamp is designed to boost the relatively weak signals from the guitar pickup and to suppress radio frequency interference. The boost comes

from a medium- $\mu$  12AY7 triode with a fully bypassed cathode. (In designs based on the 5F6-A this tube is often replaced by a high- $\mu$  12AX7 triode.) The RF suppression results from 68k grid stoppers in combination with the Miller Capacitance of the tube. There are four inputs: fully amplified normal and bright channels (the #1 inputs) and attenuated normal and bright inputs (the #2 inputs).

Except for the highest audio frequencies, where Miller Capacitance becomes a factor, the input impedance is 1 megohm at the #1 inputs and 136k at the #2 inputs. Based on a graphical analysis of the tube's AC characteristics at the DC operating point, the 12AY7 amplification factor is estimated to be 49.1 and the plate resistance is equal to 29.9k. The voltage gains are thus -32.2 and -16.1, respectively, depending on which input is used. These are not the gains that are achieved when connected to the next stage, however, because the output impedance is significant: 23k.

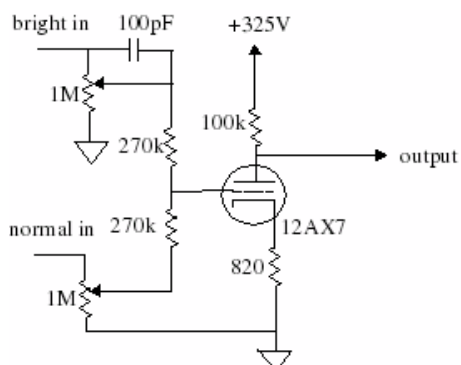


The Marshall JTM45 copies this circuit in its entirety but substitutes a high- $\mu$  12AX7 tube for greater gain. The Marshall Bluesbreaker and other early models also use the Bassman preamp. The Marshall JMP50 Model 1987 splits the normal and bright channels into separate circuits. Interestingly, however, Marshall intentionally keeps the normal channel cathode resistor at 820 ohms. It would need to double to 1.64k to provide the same DC operating point as the Bassman, because the 5F6-A resistor carries the DC current of two triodes.

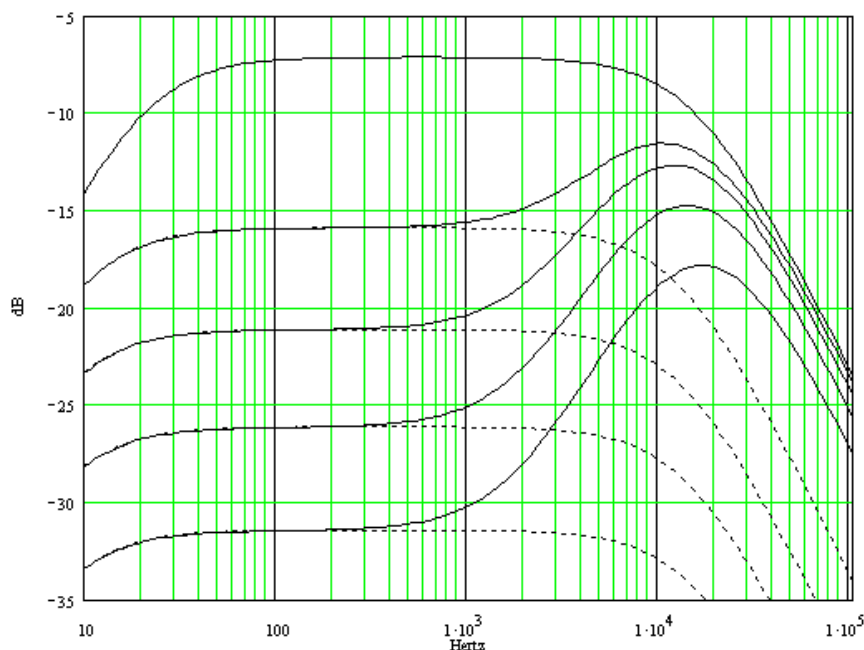
### The Marshall JMP50 Model 1987 Preamp

## The 2nd-Stage 12AX7 Voltage Amp

The next stage in the Bassman 5F6-A centers around a 12AX7 tube containing two triodes, the first of which is another voltage amplifier. Unlike the previous preamp its cathode resistor is not bypassed by a large capacitor.



The input impedance at maximum volume is 351k. From a graphical analysis of the DC operating point the triode amplification factor is estimated to be 100 and the plate resistance is 59k. This puts the voltage gain at -20.7 when the active channel's volume control is set to maximum and the inactive volume control is set to minimum. The output impedance is significant at 59k, but the input impedance of the next stage is almost infinite so the voltage gain is not significantly reduced by the connected load. The following graph (from reference 1) shows the frequency response for the bright channel input (solid) and the normal channel input (dotted) for volume settings of 100%, 50%, 25%, 12.5%, and 6.25%. This response is increased by 23 dB when we add the voltage gain of the triode.



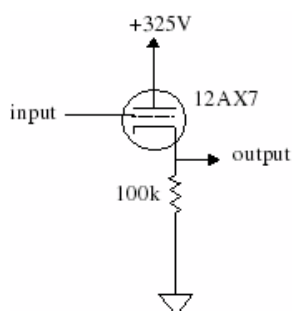
Note that at maximum volume there is no difference between the 5F6-A bright and normal channels because the volume control shorts out the 100pF bypass capacitor. The treble boost increases substantially, however, at low volume control settings.

The first Marshall JTM45 copies the Fender Bassman 5F6-A voltage amp in its entirety. Later versions increase the grid stopper resistors to 470k and provide more bypass capacitance in the bright channel input. The changes increase the difference between the two channels: the bright channel is brighter and the normal channel has more treble attenuation.

### The Marshall JMP50 Model 1987 Voltage Amp

## The 3rd-Stage 12AX7 Cathode Follower

The second 12AX7 triode is wired as a cathode follower, which has no voltage amplification but provides a low-impedance source for the tone stack that follows it. It thus acts as a buffer to isolate the voltage amplification stages from the tone stack.



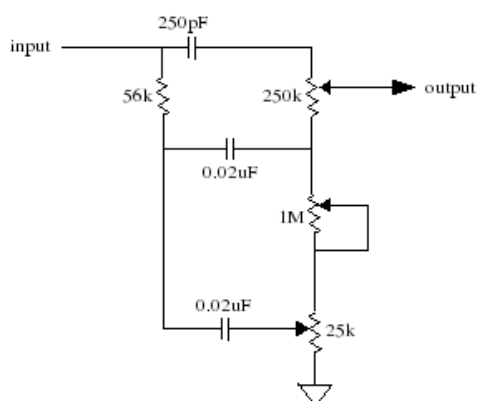
Since almost no current flows through the grid we can consider the input impedance to be infinite. Based on the DC operating point the triode amplification factor is estimated to be 93 and the plate resistance is 50k. This puts the voltage gain at +0.984, representing a slight loss. The output impedance, however, is a very low 531 ohms.

The 12AX7 cathode follower circuits in the Marshall JTM45, Bluesbreaker, and JMP50 Model 1987 are identical to the Bassman 5F6-A.

## The Tone Stack

---

The Bassman 5F6-A tone stack gives the performer the ability to control the amplifier's frequency response.



From top to bottom the potentiometers control treble, bass, and midrange. The input impedance varies depending on the tone control settings and has a worst case lower limit of 46k. There is no voltage gain in the tone stack and depending on the control settings the losses are substantial. The worst-case (highest) output impedance is 1.275 megohms. This occurs at low audio frequencies when all the tone controls are at maximum. For higher frequencies and different tone settings the output impedance is well below a megohm.

### Graphs of Fender Bassman 5F6-A Tone Stack Frequency Response

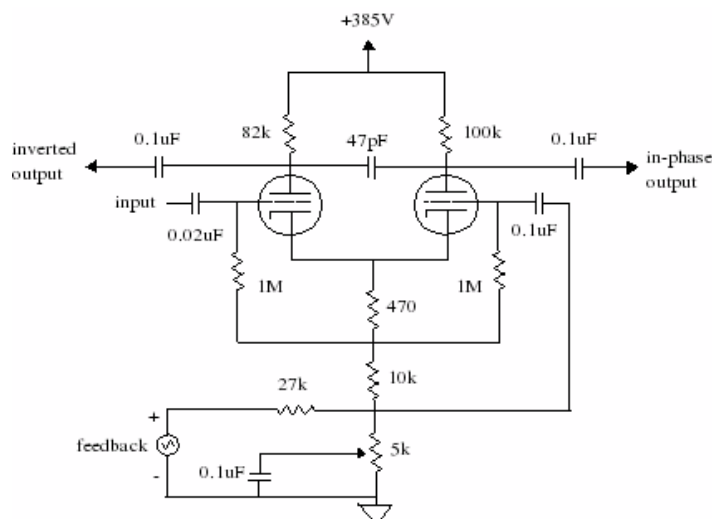
The design of the tone stack in most Marshall amplifiers is the same as in the 5F6-A, but the component values often differ. JTM45 stacks use both 270pF and 220pF capacitors instead of the Bassman's 250pF treble bypass. They also use 0.022uF instead of 0.02uF for the other bypass capacitors. Given part tolerances and the closeness of the values, however, these modifications are probably the result of component availability rather than an effort to fine tune the frequency response. The Marshall Bluesbreaker is similarly configured. The JMP50 Model 1987 substitutes 33k, 500pF, and 0.022uF instead of 56k, 250pF, and 0.02uF, which gives less midrange signal attenuation and narrows the band of frequencies defined to be midrange.

### 5F6-A versus JMP50 Tone Stacks

## The Long-Tailed-Pair Phase Inverter

---

The Bassman 5F6-A phase splitter provides further voltage amplification and creates two outputs of opposite phase to drive the push-pull power amplifier.

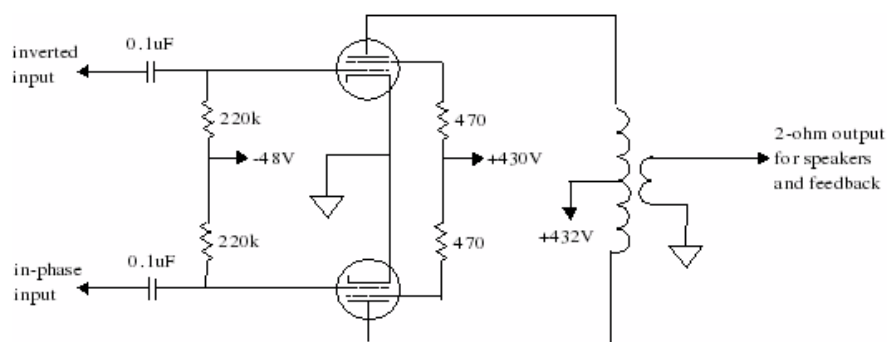


At high frequencies with the presence control at maximum the input impedance gets as low as 1.9 megohms under open-loop conditions, which is still much higher than the output impedance of the tone stack. When the presence control is at minimum the input impedance increases to more than 2.7 megohms. Negative feedback increases these values even more. Based on the DC operating point we estimate the triode amplification factors to be 101 and the plate resistances to be 57.7k. The voltage gain for the inverted output (connected to the 82k plate resistor) is then -21.9, taking into account the additional load of the push-pull power amplifier input. For the in-phase output the gain is +22.6. Feedback from the output transformer is connected to the phase splitter via a 27k resistor. The input impedance presented to the feedback signal is 31k at minimum presence and 27k at maximum presence for high frequencies. The voltage gains for the feedback input are +3.4 and -3.5 to the inverted and in-phase outputs.

The original Marshall JTM45 phase splitter is an exact copy of the Bassman 5F6-A long tailed pair. Some versions substitute 0.022uF for the 0.02uF input coupling capacitor and 4.7k instead of 5k for the presence control without significant changes in performance. The Marshall Bluesbreaker also uses this design. The JMP50 Model 1987 decreases the value of the coupling capacitors to the push-pull power amp from 0.1uF to 0.022uF.

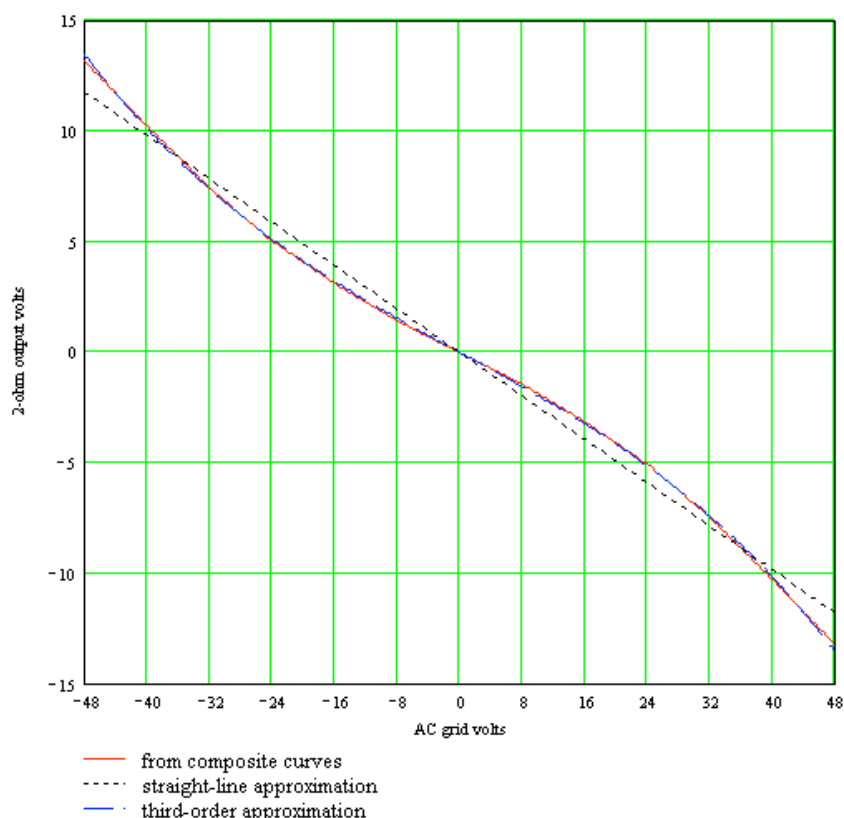
## The Push-Pull Power Amp

The Bassman 5F6-A power amplifier is a key factor in creating the amp's unique sound because its nonlinear response creates tones not found in the input signal. The 5F6-A originally shared the power load between two 5881 tubes, but new-production versions of the 6L6, which have nearly identical characteristic curves, are commonly used instead. In our analysis we use the widely available 6L6GC. The 5F6-A output transformer is model number 45249, with a 4k primary and a 2-ohm secondary.



The following graph (from reference 1) shows, for open-loop conditions, the voltage at the 5F6-A

output transformer's 2-ohm secondary versus the AC input voltage at the upper tube grid. Also shown is a straight-line approximation and a third-order approximation for the curve. By *open loop* we mean that the 27k resistor at the base of the phase splitter has been disconnected from the 2-ohm transformer output and grounded.



The Bassman's nonlinear behavior can clearly be seen in the output as deviation from a straight line. The third-order approximation, however, is almost indistinguishable, which indicates that most of the nonlinearity can be described by the product of a constant and the cube of the AC input voltage. The output voltage as a function of the input voltage  $v$  is thus closely approximated by  $Av^3 + Cv$ , where  $A$  and  $C$  are constants. We used linear regression to estimate the values of the constants at two operating extremes: no power supply voltage sag and maximum power supply voltage sag. The first condition occurs when the amplifier has been operating at very low power levels and then experiences a sudden increase to maximum power. The second condition represents the steady-state condition where the amplifier has been operating at maximum power long enough for the power supply voltage to sag to its minimum level. At maximum sag we conclude that  $A = -4.2 \times 10^{-5}$  and  $C = -0.17$ . When there is no sag  $A = -2.9 \times 10^{-5}$  and  $C = -0.25$ . Voltage sag thus increases the magnitude of the nonlinear coefficient  $A$  and decreases the magnitude of the linear coefficient  $C$ . Sag therefore increases nonlinear distortion.

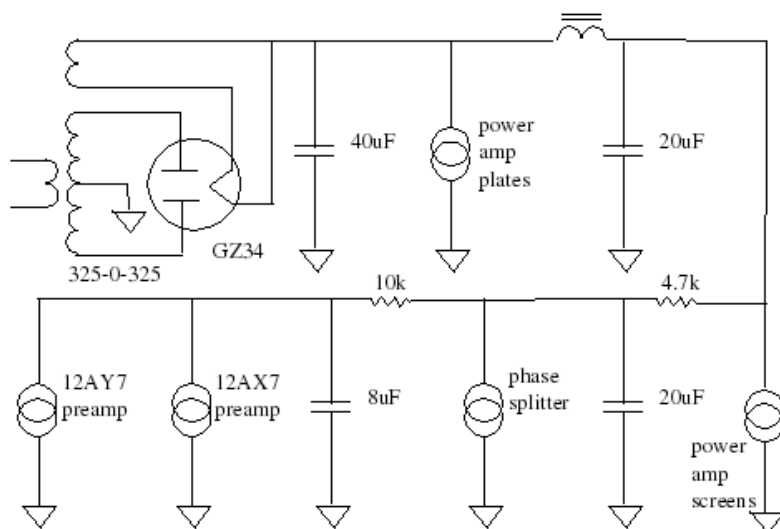
Using a third-order approximation, the 5F6-A's open-loop, third-harmonic distortion is 9 percent (maximum supply voltage sag) and 5 percent (no sag). Under closed-loop conditions with the presence control at minimum the Bassman's harmonic distortion is significantly less due to negative feedback.

The Marshall JTM45 power amp is a direct copy of the Bassman 5F6-A circuit except for one very important change: the negative feedback signal is taken from the 16-ohm transformer output instead of the 2-ohm output. This almost triples the feedback voltage, which reduces nonlinear distortion and flattens the amplifier's frequency response at the cost of less overall gain. Later Marshalls, including the JMP50 Model 1987, use EL34 pentodes, so although the push-pull, class AB circuit design is the same (except for component values and supply voltages), the tube change

dramatically alters its characteristics.

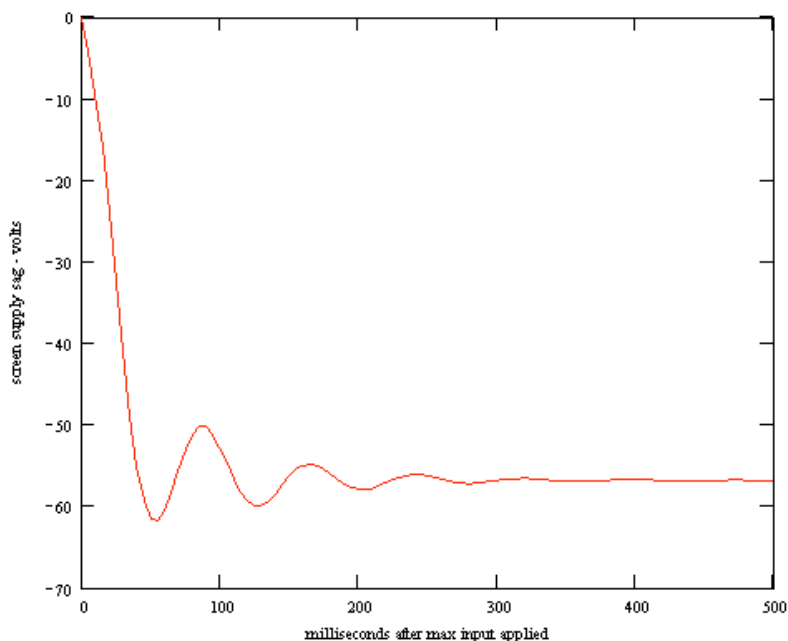
## The Power Supply

The Fender Bassman 5F6-A power supply consists of a GZ34 full-wave rectifier tube and a series of low-pass filters that supply DC power to each of the amplifier stages. The two output plates are by far the biggest current consumers. Because the pentodes are operating in push-pull they are relatively immune from power supply ripple and are placed the furthest upstream in the filter chain where the most ripple exists. The preamps, with their low-level audio signals, are the most susceptible to hum and thus receive the most filtering.

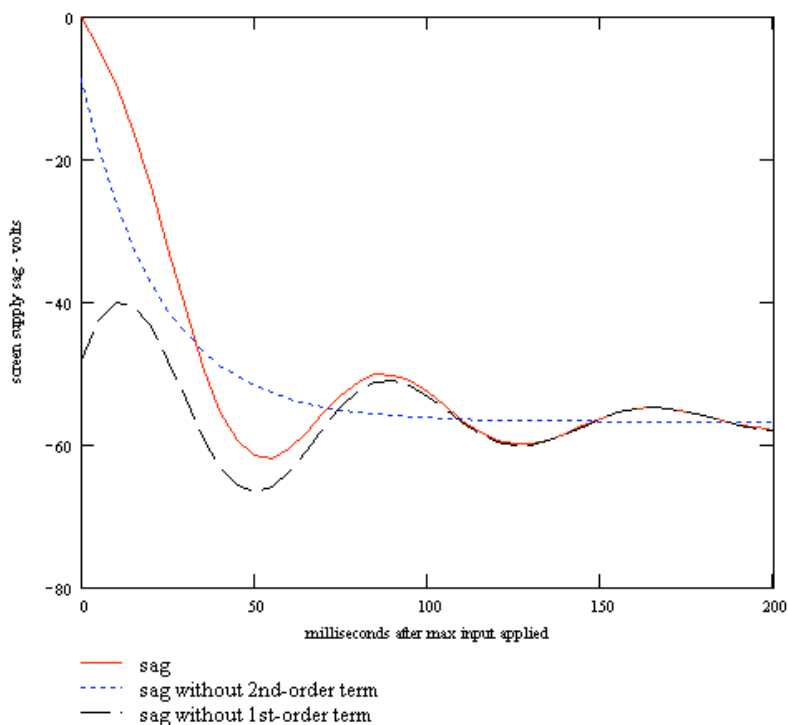


Because the 5F6-A power supply uses a full-wave rectifier, the fundamental frequency of the AC hum is 120 Hz. At that frequency there is 42dB of hum attenuation at the pentode plate supplies, 83dB at the screen supplies, 120dB at the phase splitter plate supplies, and 156dB at the preamp plate supplies. There is less attenuation if the amplifier is powered by 50Hz, as would be the case in Europe.

A sudden increase in audio power level, from zero signal to maximum power, causes the 5F6-A class AB power amp to draw much more current. Because of resistance in the Bassman's power supply transformer windings and in the GZ34 rectifier, the increased current load causes the DC output voltage to drop. The power supply's large filter capacitors and choke are able to temporarily supply current to the screens and plates, which causes the voltage to gradually sag over time. Their reaction time in response to a change in load is an important characteristic of the amplifier. The following graph (from reference 1) shows how the DC screen supply voltage sags during the first half second in response to an instantaneous increase in signal amplitude from zero signal to maximum power.



The Bassman's response consists of three components added together. The first component represents the steady-state screen supply voltage sag at maximum power. The second is a transient component that decreases exponentially with time. It has a time constant of 0.022, so after 22 milliseconds it is reduced to 37 percent of its start value. The third component, representing an underdamped condition, decreases exponentially at a slower rate, 0.72, and has a damped frequency of oscillation of 13 Hz. The oscillation is caused by the interaction of the choke with the filter capacitors. The three separate components are broken out in the next graph (also from reference 1).



The graph shows the steady-state plus first transient, steady-state plus second transient, and total response over the first 200 milliseconds.

The Bassman 5F6-A power transformer is model number 8087. It has a 325-0-325 secondary,

which means that it has two opposite phases that are 325 volts RMS (460 volts peak) and a center tap that is connected to ground. The transformer has separate secondary windings that supply 1.9A at 5 volts to the GZ34 filament and 2.7A at 6.3 volts to the triodes and pentodes. The 5F6-A choke is model number 14684.

The Marshall JTM45 power supply is identical to the 5F6-A except for component values. The grid bias supply in particular is fixed and taken from the same transformer tap as the Bassman. The JMP50 Model 1987, however, shifts the grid supply to one phase of the high-voltage secondary, eliminating the need for a lower-voltage tap, and adds a variable resistor to enable the bias voltage to be adjusted.

### [The Marshall JMP50 Model 1987 Grid Bias Supply](#)

## References

---

<sup>1</sup>Richard Kuehnel, [Circuit Analysis of a Legendary Tube Amplifier: The Fender Bassman 5F6-A](#), 2nd Ed., (Seattle: Pentode Press, 2005).

<sup>2</sup>Michael Doyle, [The History of Marshall](#), (Milwaukee: Hal Leonard Corp., 1993).

---

[Home](#) | [Legal Notice](#) | [Contact](#)  
Copyright © 2005-2009 Pentode Press



## DISCRETIZATION OF THE '59 FENDER BASSMAN TONE STACK

David T. Yeh, Julius O. Smith

Center for Computer Research in Music and Acoustics (CCRMA)  
Stanford University, Stanford, CA  
{dtyeh|jos}@ccrma.stanford.edu

### ABSTRACT

The market for digital modeling guitar amplifiers requires that the digital models behave like the physical prototypes. A component of the iconic Fender Bassman guitar amplifier, the tone stack circuit, filters the sound of the electric guitar in a unique and complex way. The controls are not orthogonal, resulting in complicated filter coefficient trajectories as the controls are varied. Because of its electrical simplicity, the tone stack is analyzed symbolically in this work, and digital filter coefficients are derived in closed form. Adhering to the technique of virtual analog, this procedure results in a filter that responds to user controls in exactly the same way as the analog prototype. The general expressions for the continuous-time and discrete-time filter coefficients are given, and the frequency responses are compared for the component values of the Fender '59 Bassman. These expressions are useful implementation and verification of implementations such as the wave digital filter.

### 1. INTRODUCTION

#### 1.1. Motivation

The guitar amplifier is an essential component of the electric guitar sound, and often musicians collect several amplifiers for their tonal qualities despite the space they occupy. As digital signal processors (DSP) continue to improve in performance, there is great interest in replacing expensive and bulky vacuum tube guitar amplifiers with more flexible and portable digital models. A digital model of a guitar amplifier allows a variety of sounds associated with different amplifiers to be selected from a single amplifier unit. One company, Line 6 bases its main product line upon this concept, and other companies such as Roland (Boss), Korg (Vox), Harman International (Digitech) have competing products.

Most commercially viable digital guitar processing products use simplified models of the distortion and filters to reduce DSP power consumption and reduce manufacturing costs. The distortion is typically a nonlinear transfer curve, accompanied by digital filtering that is manually tuned to match the sound of a famous guitar amplifier.

With no pressure to produce a commercially successful product, this research takes a different approach. The goal of this research is to see how accurate a sound can be achieved through careful physical modeling of the vacuum tube amplifier and to provide a physical basis for the digital model and parameters. Because the tone stack is a passive, linear component, it is a straightforward starting point.

#### 1.2. Properties of the tone stack

Commonly found in many guitar amplifiers, especially those that derive from the Fender design, the tone stack filters the signal of

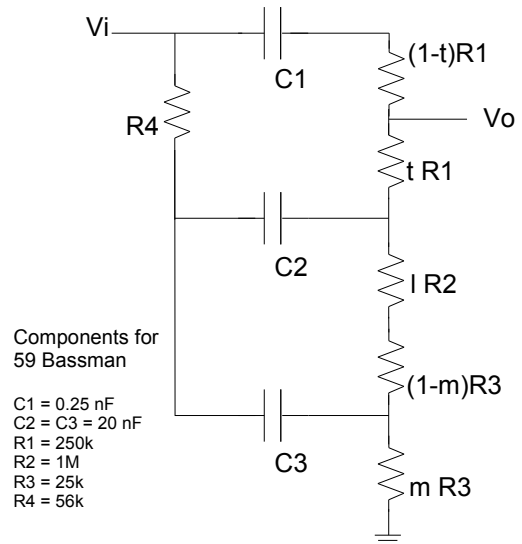


Figure 1: Tone stack circuit with component values.

the guitar in a unique and non-ideal way. The user can adjust Treble, Middle, and Bass controls to modify the gain of the respective frequency bands. However, these controls are not orthogonal, and changing some controls affects the other bands in a complex way.

The full Bassman schematic can be easily found online [1] and in guitar amplifier books. While other guitar amplifiers may vary slightly, in the Bassman type designs, the tone stack is found after the preamplifier stages and before the phase splitter. In good designs, the tone stack is preceded by a cathode follower to buffer the input and reduce variations in frequency response due to loading. Typically this presents a  $1k\Omega$  load to the input and the phase splitter stage presents a  $1M\Omega$  load to the output.

The Fender '59 Bassman tone stack circuit is shown in Fig. 1. The Treble, Middle, and Bass knobs are potentiometers, which have been modeled here as parameterized resistors. The Treble and Middle controls use linear potentiometers, while the Bass control uses a logarithmic taper potentiometer. In this paper,  $t$  and  $m$  correspond to the Treble and Middle controls and range in value from  $[0, 1]$ . The Bass control,  $l$ , also ranges from  $[0, 1]$ , but is swept logarithmically.

### 1.3. Related work

Fender Musical Instruments has a patent to simulate various tone stacks using an active analog filter and an interpolation scheme to extract the filter coefficients [2]. Line 6 also models the behavior of the Bassman tone stack as indicated in the BassPODxt manual. However, their implementation is proprietary knowledge. An open source guitar effects plug-in suite for Linux, CAPS [3], uses shelving filters instead of the tone stack.

Previous works have analyzed the tone stack using numerical circuit analysis techniques. This involves setting up the nodal equations as a matrix and inverting it or performing Gaussian elimination to find the solution. For example, the Tone Stack Calculator from Duncan Amps will plot the frequency response of various tone stacks given the control settings [4]. Kuehnel in his book analyzed the mesh equations of the tone stack, using low frequency and high frequency circuit approximations [5]. He also compares these simplified equations to the numerical solutions solved by inverting the matrix of the mesh equations. While the approximations make the circuit analysis more tractable, they do not reduce the order of the equations and do not make the discretization of the filter any easier.

Because the tone stack is a third-order passive network of resistors and capacitors (RC), its filter coefficients can be derived and modeled exactly in the digital domain as shown later. The approach taken here is to find the continuous time transfer function of the circuit analytically and to discretize this by the bilinear transformation. This provides a means of updating the digital filter coefficients based upon changes to the tone controls.

The passive filter circuit also is suited to implementation as a wave digital filter (WDF)[6]. This approach can easily model standard components such as inductors, capacitors, and resistors. The analytical form derived here can be used for comparison with and verification of the WDF implementation.

## 2. DISCRETIZATION PROCEDURE

### 2.1. Symbolic Circuit Analysis

Because this is a relatively simple circuit, it is amenable to exact symbolic analysis by mathematical Computer Aided Design (CAD) software such as Mathematica (Wolfram Research, Inc., Champaign, IL). The filter coefficients can thus be found without any approximations. Performing symbolic nodal analysis on this circuit yields the following input/output transfer function  $H(s) = V_o(s)/V_i(s)$ , where  $V_o$  is the output and  $V_i$  is the input as in Fig. 1.

$$H(s) = \frac{b_1 s + b_2 s^2 + b_3 s^3}{a_0 + a_1 s + a_2 s^2 + a_3 s^3}, \quad (1)$$

where

$$b_1 = tC_1R_1 + mC_3R_3 + l(C_1R_2 + C_2R_2) + (C_1R_3 + C_2R_3),$$

$$\begin{aligned} b_2 = & t(C_1C_2R_1R_4 + C_1C_3R_1R_4) - m^2(C_1C_3R_3^2 + C_2C_3R_3^2) \\ & + m(C_1C_3R_1R_3 + C_1C_3R_3^2 + C_2C_3R_3^2) \\ & + l(C_1C_2R_1R_2 + C_1C_2R_2R_4 + C_1C_3R_2R_4) \\ & + lm(C_1C_3R_2R_3 + C_2C_3R_2R_3) \\ & + (C_1C_2R_1R_3 + C_1C_2R_3R_4 + C_1C_3R_3R_4), \end{aligned}$$

$$\begin{aligned} b_3 = & lm(C_1C_2C_3R_1R_2R_3 + C_1C_2C_3R_2R_3R_4) \\ & - m^2(C_1C_2C_3R_1R_3^2 + C_1C_2C_3R_3^2R_4) \\ & + m(C_1C_2C_3R_1R_3^2 + C_1C_2C_3R_3^2R_4) \\ & + tC_1C_2C_3R_1R_3R_4 - tmC_1C_2C_3R_1R_3R_4 \\ & + tlC_1C_2C_3R_1R_2R_4, \end{aligned}$$

$$a_0 = 1,$$

$$\begin{aligned} a_1 = & (C_1R_1 + C_1R_3 + C_2R_3 + C_2R_4 + C_3R_4) \\ & + mC_3R_3 + l(C_1R_2 + C_2R_2), \end{aligned}$$

$$\begin{aligned} a_2 = & m(C_1C_3R_1R_3 - C_2C_3R_3R_4 + C_1C_3R_3^2 \\ & + C_2C_3R_3^2) + lm(C_1C_3R_2R_3 + C_2C_3R_2R_3) \\ & - m^2(C_1C_3R_3^2 + C_2C_3R_3^2) + l(C_1C_2R_2R_4 \\ & + C_1C_2R_1R_2 + C_1C_3R_2R_4 + C_2C_3R_2R_4) \\ & + (C_1C_2R_1R_4 + C_1C_3R_1R_4 + C_1C_2R_3R_4 \\ & + C_1C_2R_1R_3 + C_1C_3R_3R_4 + C_2C_3R_3R_4), \end{aligned}$$

$$\begin{aligned} a_3 = & lm(C_1C_2C_3R_1R_2R_3 + C_1C_2C_3R_2R_3R_4) \\ & - m^2(C_1C_2C_3R_1R_3^2 + C_1C_2C_3R_3^2R_4) \\ & + m(C_1C_2C_3R_3^2R_4 + C_1C_2C_3R_1R_3^2 \\ & - C_1C_2C_3R_1R_3R_4) + lC_1C_2C_3R_1R_2R_4 \\ & + C_1C_2C_3R_1R_3R_4, \end{aligned}$$

where  $t$  is the Treble (or “top”) control,  $l$  is the Bass (or “low”) control, and  $m$  is the “middle” control.

### 2.2. Verification with SPICE circuit simulation

To verify the correctness of this expression, Figs. 2 and 3 compare the frequency response with the result from the AC analysis of SPICE<sup>1</sup> simulation at the settings  $t = m = l = 0.5$ . The plots show an exact match, verifying that Eqn. 1 is a complete and exact expression for the transfer function of the tone stack. SPICE simulation also determined that the frequency response was unaffected by the typical loading of  $1k\Omega$  at the input and  $1M\Omega$  at the output.

### 2.3. Discretization by Bilinear Transform

The continuous time transfer function was discretized by the bilinear transformation. Substituting  $s = c\frac{1-z^{-1}}{1+z^{-1}}$  in (1) using Mathematica yields

$$H(z) = \frac{B_0 + B_1z^{-1} + B_2z^{-2} + B_3z^{-3}}{A_0 + A_1z^{-1} + A_2z^{-2} + A_3z^{-3}} \quad (2)$$

where

$$\begin{aligned} B_0 = & -b_1c - b_2c^2 - b_3c^3, \\ B_1 = & -b_1c + b_2c^2 + 3b_3c^3, \\ B_2 = & b_1c + b_2c^2 - 3b_3c^3, \\ B_3 = & b_1c - b_2c^2 + b_3c^3, \\ A_0 = & -a_0 - a_1c - a_2c^2 - a_3c^3, \\ A_1 = & -3a_0 - a_1c + a_2c^2 + 3a_3c^3, \\ A_2 = & -3a_0 + a_1c + a_2c^2 - 3a_3c^3, \\ A_3 = & -a_0 + a_1c - a_2c^2 + a_3c^3. \end{aligned}$$

<sup>1</sup><http://bwrc.eecs.berkeley.edu/Classes/lcBook/SPICE/>

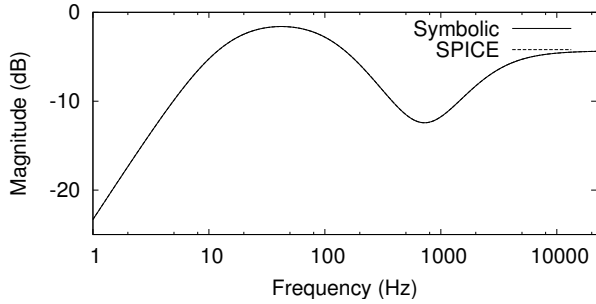


Figure 2: Comparison of magnitude response between analytical expression and SPICE for  $t = l = m = 0.5$ .

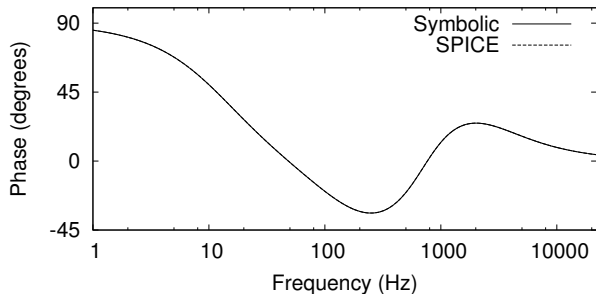


Figure 3: Comparison of phase response between analytical expression and SPICE for  $t = l = m = 0.5$ .

We used  $c = 2/T$ , which is ideal for frequencies close to DC.

### 3. ANALYSIS OF RESULTS

#### 3.1. Comparison of continuous- and discrete- time responses

Figs. 4–6 show the discrete- and continuous-time transfer functions compared for various settings of  $t$ ,  $m$ , and  $l$ . Each figure shows a different setting of  $l$ , and each sub-figure shows a different setting of  $m$ . In each plot, the treble control,  $t$ , was swept from 0.0001 to 0.5 to 0.9999 and can be distinguished by the corresponding increase in high frequency response.

The discretized filter used a sampling frequency of 44.1 kHz as typical for audio systems. The plots for  $f_s = 44.1$  kHz show an excellent match through 10 kHz. The discrete and continuous plots are practically indistinguishable, with some deviations at the higher frequencies, as expected with the bilinear transform.

Because commercial guitar processing units use a lower sampling rate for cost savings, Figs. 7–9 show the same plots as above with  $f_s$  reduced to 20 kHz. These curves deviate slightly more from  $H(s)$  at high frequencies, but exhibit the same trends as before.

The errors, defined as the difference between the dB values of  $H(s)$  and  $H(z)$  at each frequency, are plotted in Fig. 10 for  $f_s = 20$  kHz and  $f_s = 44.1$  kHz (abbreviated as 44k) for the settings of  $t$ ,  $m$ , and  $l$  that give the worst case results. The error is only meaningful for frequencies up through  $f_s/2$ .

The curves for  $t = 0.5, m = 0, b = 1$  are characteristic of tone settings that give a high pass response and have error within 0.5 dB for both cases of  $f_s$ .

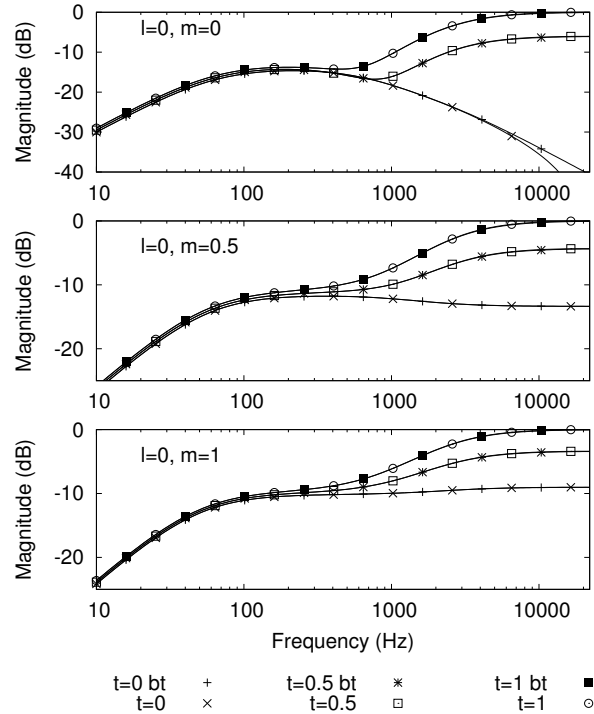


Figure 4: Comparison of filter magnitude response between original and discretized ( $f_s = 44.1$  kHz) filters,  $l = 0$ .

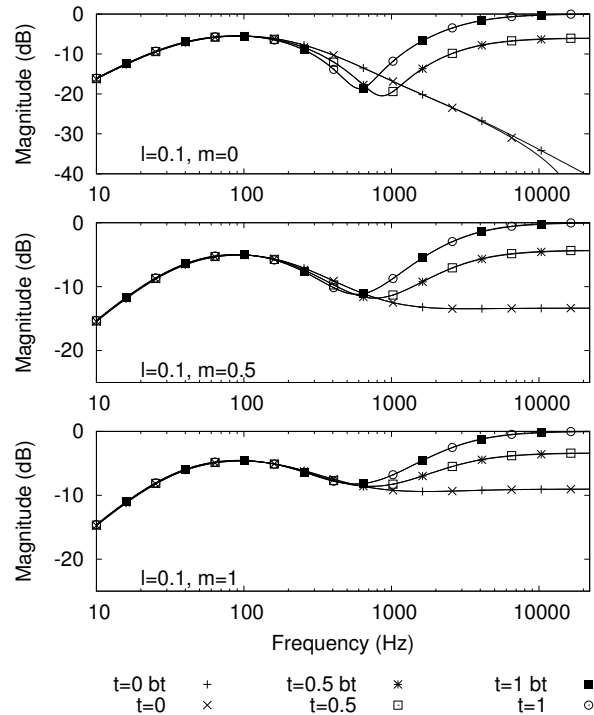


Figure 5: Comparison of filter magnitude response between original and discretized ( $f_s = 44.1$  kHz) filters,  $l = 0.1$ .

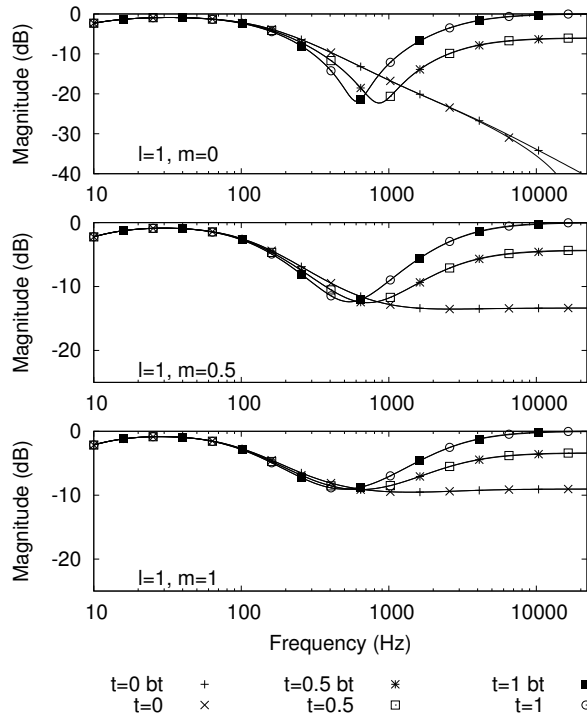


Figure 6: Comparison of filter magnitude response between original and discretized ( $f_s = 44.1$  kHz) filters,  $l = 1$ .

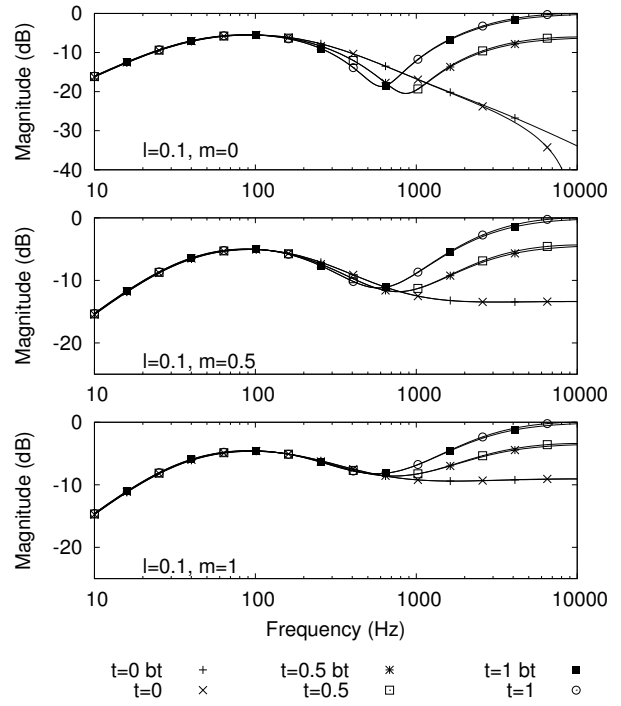


Figure 8: Comparison of filter magnitude response between original and discretized ( $f_s = 20$  kHz) filters,  $l = 0.1$ .

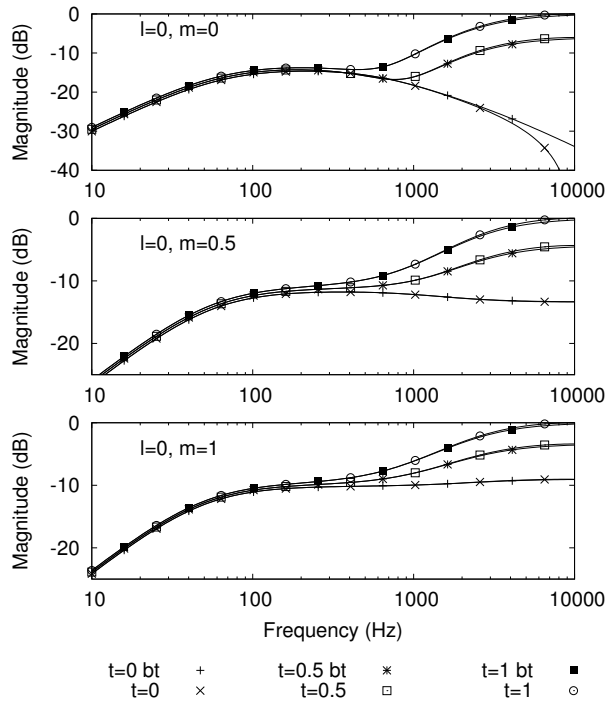


Figure 7: Comparison of filter magnitude response between original and discretized ( $f_s = 20$  kHz) filters,  $l = 0$ .

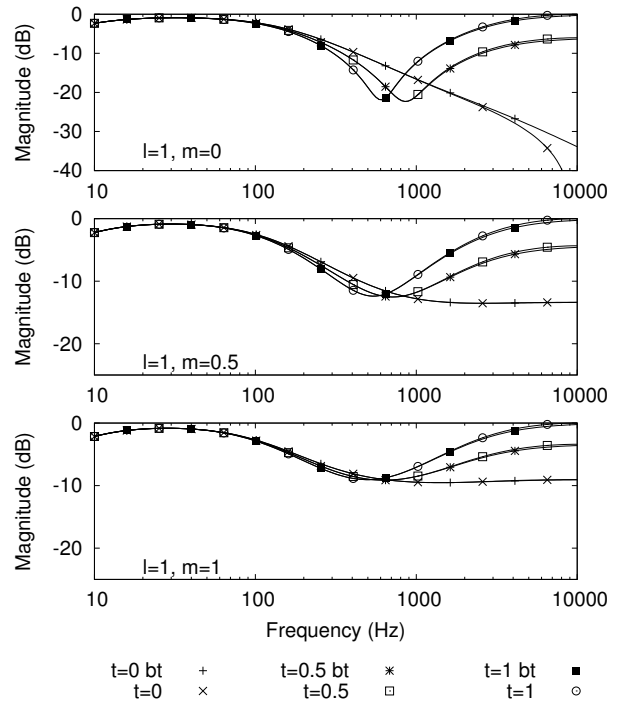


Figure 9: Comparison of filter magnitude response between original and discretized ( $f_s = 20$  kHz) filters,  $l = 1$ .

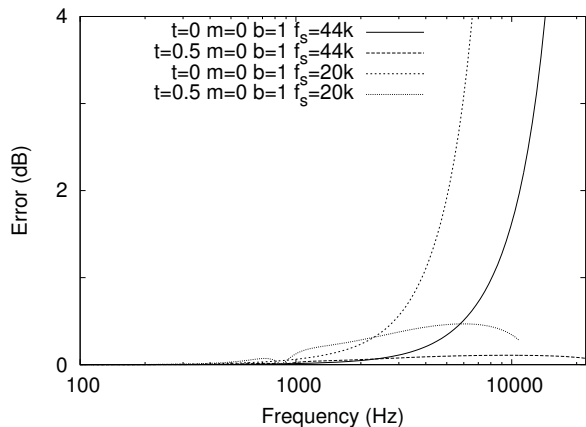


Figure 10: Error as difference between dB values of  $H(s)$  and  $H(z)$ , for  $f_s = 20$  and  $44.1$  kHz, and the noted tone settings.

The curves for  $t = 0, m = 0, b = 1$  are characteristic of settings that give a low pass response and exhibit a rapidly increasing error as frequency increases because the bilinear transform maps the null at infinite frequency to  $f_s/2$ . The error rises to 3 dB at roughly 6 kHz for  $f_s = 20$  kHz, and at 13 kHz for  $f_s = 44.1$  kHz. Because of the low pass nature of these responses, the errors occur at frequencies where the magnitude is at least 10-20 dB lower than its peak value, making them perceptually less salient. Also, given that the frequency response of a typical guitar speaker is from 100 Hz to 6000 Hz, the deviations at higher frequencies would be inconsequential.

### 3.2. Implications of system poles and zeros for filter implementation

The plots exhibit the complex dependence of the frequency response upon the tone controls. The most obvious effect is that changes in the *Middle* control also affect the treble response. The analytical form of the transfer function provides a way to find the poles and zeros of the system as the settings are varied and gives insight into how the filter could be simplified to facilitate the implementation while maintaining accuracy.

Note that the tone stack is an entirely passive circuit composed of resistors and capacitors. This implies that the three poles of this system are all real. There is a zero at DC, leaving a pair of zeros that may be complex depending on the control settings. This also implies that the tone stack cannot be a resonant circuit although the pair of imaginary zeros can set up an anti-resonance as evident in the notch seen in the frequency response plots.

Also note from Eqn. (1) that none of the coefficients of the denominator depends on the treble control,  $t$ . The treble control therefore does not control the modes of the circuit but only adjusts the position of the zeros. This circuit can be decomposed into a weighted sum of terms that correspond to each mode by the partial fraction expansion. From this perspective, the treble control only affects the weighting of the different modes, but not the pole location of each mode. The poles are controlled exclusively by the bass and middle knobs.

This insight suggests possible alternate filter topologies. Instead of implementing the filter directly as a single third-order filter, one could equivalently use series and parallel combinations of

lower order filters. Understanding the poles and zeros of the system, one could make simplifying assumptions, ignoring terms that have little impact on the locations of the poles and zeros.

One implementation would be to find the partial fraction expansion of the transfer function using the expression given and precompute the poles, residues, and direct terms based upon the three-dimensional input space of the tone controls. These terms can be interpolated in the input space and used in the parallel filter structure that arises from the partial fraction expansion.

The existence of an analytical expression for the poles and zeros also informs the choice of  $c$  in the bilinear transform. The analytical expression allows the computation of frequency domain features such as local maxima or anti-resonance notches to be matched in the discrete-time domain.

## 4. CONCLUSIONS

This work shows that the Fender tone stack can be parameterized exactly in the discrete-time domain and that the bilinear transform provides an outstanding frequency mapping for reasonable sampling rates. The transfer function for the physical tone stack was found as a function of its control parameters and component values using symbolic math software. This analysis provides a formula for updating the digital tone stack coefficients in a way that exactly emulates the physical circuit. The symbolic form of the transfer function also allows easy determination of the poles and zeros of the system and guides the design of a filter with simplified coefficients.

Further work remains to factor the expression for the tone stack frequency response and find a structure with simpler expressions for updating the filter. One possible implementation is the wave digital filter. A real-time implementation of the tone stack is also in progress.

## 5. ACKNOWLEDGEMENTS

David Yeh is supported by the NDSEG fellowship. Thanks to Tim Stilson for help with root loci.

## 6. REFERENCES

- [1] Ampwares, "5F6-A schematic," Retrieved June 29th, 2006, [Online] [http://www.ampwares.com/ffg/bassman\\_narrow.html](http://www.ampwares.com/ffg/bassman_narrow.html).
- [2] D. V. Curtis, K. L. Chapman, C. C. Adams, and Fender Musical Instruments, "Simulated tone stack for electric guitar," United States Patent 6222110, 2001.
- [3] T. Goetze, "caps, the C Audio Plugin Suite," Retrieved June 29th, 2006, [Online] <http://quitte.de/dsp/caps.html>.
- [4] Duncan Amps, "Tone stack calculator," Retrieved June 29th, 2006, [Online] <http://www.duncanamps.com/tsc/>.
- [5] R. Kuehnel, *Circuit Analysis of a Legendary Tube Amplifier: The Fender Bassman 5F6-A*, 2nd ed. Seattle: Pentode Press, 2005. [Online]. Available: <http://www.pentodepress.com/contents.html>
- [6] A. Fettweis, "Wave digital filters: Theory and practice," *Proc. IEEE*, vol. 74, pp. 270–327, Feb. 1986.